Final Report

Physics of Complex Networks: Structure and Dynamics

Università degli Studi di Padova

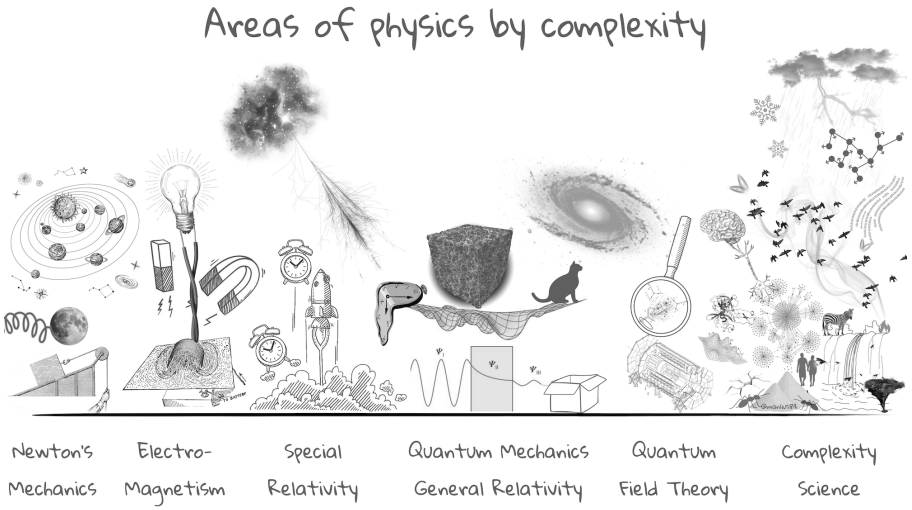

Projects Report: 15, 44

Tuscano Alessio

Last update: February 16, 2026

Contents

1 | Task 15: Self-Organized Criticality on Networks

1.1 | Framework

We simulate the Bak–Tang–Wiesenfeld (BTW) sandpile on a network with N nodes. Each node i carries an integer load $z_i \in \{0, 1, 2, \dots\}$ and a threshold $z_c(i)$. At each driving step one grain is added to a uniformly random node; the system then relaxes via topplings. On a generic graph we set $z_c(i) = k_i$ (degree threshold), so a toppling at i sends exactly one grain to each of its k_i neighbors:

$$z_i \leftarrow z_i - k_i, \qquad z_j \leftarrow z_j + 1 \quad \forall j \in \partial i. \tag{1.1}$$

On finite networks without open boundaries, some form of dissipation is needed for a stationary state. We use *per-grain* dissipation [6]: each outgoing grain is independently lost with probability f, so that on average a fraction f of the redistributed load disappears per toppling. An *avalanche* is the full relaxation triggered by one grain addition. We measure: size S (total topplings), duration T (parallel-update waves), and area A (distinct toppled nodes).

1.2 | SOC on single topologies

Mean-field baseline (Bonabeau). In the random-neighbor (annealed) model [2] each toppling redistributes grains to k nodes chosen uniformly at random rather than along fixed edges. This removes quenched structural correlations and yields mean-field exponents: the avalanche-size distribution follows $P(S) \sim S^{-3/2}$, i.e. the CCDF scales as $P(S \geq s) \sim s^{-1/2}$. We verify this numerically with $N = 20\,000$, $k = 4$, and dissipation $\varepsilon \in \{10^{-3}, 3\times10^{-3}, 10^{-2}\}$ (3×10^5 driving steps each, 2×10^4 transient discarded). Fig. 1.1 (left) confirms the expected power-law tail; smaller ε extends the scaling regime before the finite-size cutoff.

Quenched scale-free topology (Goh et al.). On a quenched scale-free network generated with the static model [6] (mean degree $\langle k \rangle = 4$, degree threshold $z_c(i) = k_i$), the avalanche exponent depends on the degree exponent γ. Goh et al. predict $\tau_A = \gamma/(\gamma - 1)$ for $2 < \gamma < 3$ (non-mean-field) and $\tau_A = 3/2$ for $\gamma \geq 3$ (mean-field), with τ_A defined via $P(A) \sim A^{-\tau_A}$.

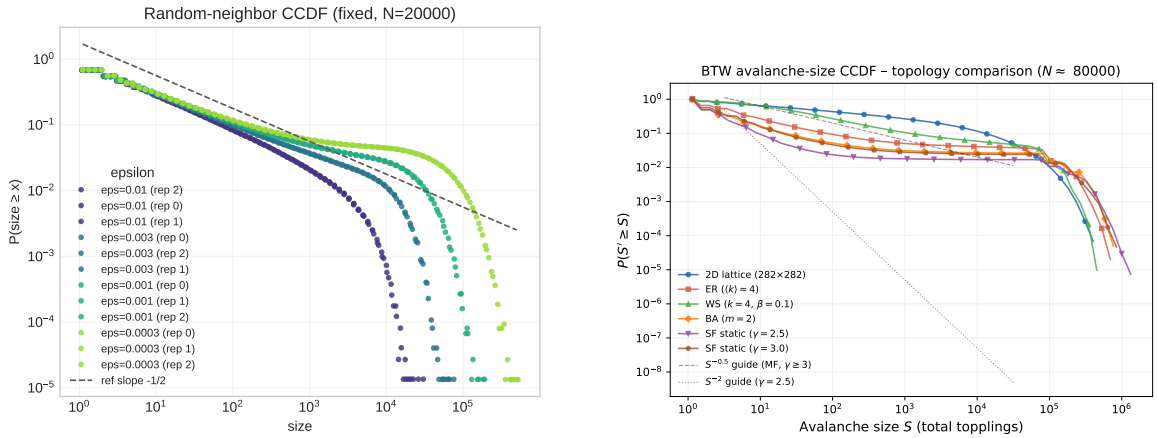

Figure 1.1: Left: annealed random-neighbor model ($N = 20\,000$, $k = 4$) avalanche-size CCDF for three dissipation rates; dashed line marks the mean-field slope $-1/2$. Right: avalanche-size CCDF on six quenched topologies ($N \approx 80\,000$, degree threshold, $f = 10^{-4}$); homogeneous networks cluster near the MF guide while heterogeneous ones (BA, SF) show progressively steeper tails.

Topology comparison. We run the BTW sandpile ($z_c(i) = k_i$, per-grain dissipation $f = 10^{-4}$, 5×10^5 steps, 5×10^4 transient) on six synthetic topologies with $N \approx 80\,000$: a 2D square lattice (282×282, open boundary), an Erdős–Rényi (ER) random graph ($\langle k \rangle \approx 4$), a Watts–Strogatz (WS) small-world network ($k = 4$, rewiring $\beta = 0.1$), a Barabási–Albert (BA) preferential-attachment network ($m = 2$), and two scale-free (SF) networks from the static model with $\gamma = 2.5$ and $\gamma = 3.0$. Fig. 1.1 (right) overlays the resulting avalanche-size CCDFs. The homogeneous topologies (lattice, ER, WS) cluster near the mean-field $S^{-1/2}$ guide, confirming that low degree variance leaves scaling unaffected. In contrast, the heterogeneous networks (BA, SF) should show markedly steeper tails: degree-heterogeneity concentrates load on hubs, producing more frequent moderate cascades but suppressing the very large ones. Goh et al. predict $\tau_S = \gamma/(\gamma - 1) = 5/3$ for $\gamma = 2.5$ (CCDF $\sim S^{-2/3}$) and MF recovery for $\gamma \geq 3$ [6]. The qualitative ordering is confirmed—heterogeneous curves are steeper—but the quantitative separation is weaker than in the original paper, where dissipation occurs through a *sink node* connected to all vertices (open boundary) rather than through per-grain stochastic loss. With per-grain dissipation the effective loss rate of a hub scales as $\sim f k_i$, disproportionately damping high-degree nodes and partially washing out the topology-dependent exponent shift.

1.3 | SOC with interdependence

Coupled sandpiles and large cascades. We now consider two modules A and B, each with $N = 2000$ nodes, connected by a sparse set of inter-module edges (bridges). Each node in module A is independently selected as a bridge endpoint with probability p; the same number of nodes is drawn from B and paired uniformly at random [3]. Because the threshold is degree-based, adding a bridge to node i raises its threshold $z_c(i)$ by one (higher local stability), but also creates a new pathway for load to propagate between modules.

Following [3], we classify events by whether a *large* cascade occurs in module A:

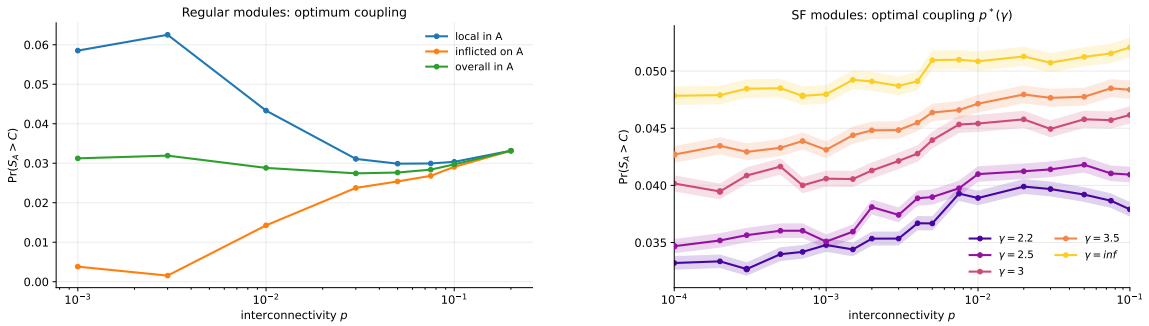

Figure 1.2: Probability of a large cascade in module A versus coupling p. Left: regular modules ($z = 3$) showing the local/inflicted/overall decomposition. Right: SF modules for several γ; lower γ shifts the minimum to smaller p.

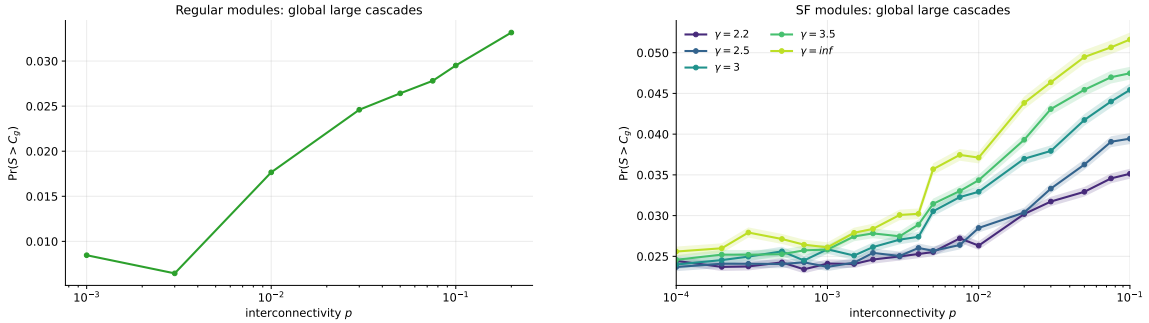

Figure 1.3: Probability of a *global* large cascade ($S > C_g = 2000$) versus p. The non-monotonic shape persists, supporting the "optimal coupling" interpretation rather than a cutoff artifact.

$S_A > C$ with $C = N/2 = 1000$. We also track *global* cascades ($S > C_g$, $C_g = N = 2000$). Dissipation is per-toppling with $f = 0.01$; each simulation runs 5×10^5 steps with 5×10^4 transient. The "regular" modules are random 3-regular graphs; the scale-free modules use the static model with tunable γ (taking $\gamma = \infty$ recovers a homogeneous degree distribution near the ER limit). In the SF panels, shaded bands show 95% Wilson-score confidence intervals from aggregated event counts across 2 replicates.

Fig. 1.2 separates cascades that remain within A (local) from those triggered by activity arriving from module B (inflicted), and their union (any large in A). At small p, the few bridges divert load away from module A, suppressing its largest within-module cascades. At large p, bridges raise node thresholds (making individual topplings less frequent) but simultaneously enable inflicted cascades: when a node does topple, it can inject load into the other module. The competition between these two effects can produce a non-trivial optimum p^* at which large cascades are least likely [3].

Global cascades (Fig. 1.3) show the same qualitative non-monotonic pattern. Small coupling suppresses the largest events; strong coupling enables system-wide propagation. For the regular-module case, the optimum lies near $p^* \approx 0.01$, consistent with [3]. In the SF extension, the optimum p^* shifts to smaller values for lower γ: heterogeneous networks are more sensitive to inter-module coupling, likely because high-degree hubs act as efficient conduits for cross-module load transfer once bridges reach them.

2 | Task 44: Social Connectedness Index II

2.1 | Dataset and network construction

The Social Connectedness Index (SCI) by Meta quantifies the intensity of Facebook friendship ties between pairs of administrative regions [1]. For regions i, j the published score is

$$\mathrm{SCI}_{ij} \propto \frac{F_{ij}}{U_i\, U_j},$$

where F_{ij} counts cross-region friendships and U_i, U_j are the Facebook-user populations; values are rescaled within each layer to $[1, 10^9]$ (`scaled_sci`) [7]. We use the SCI II release (reference period 2025-12-26 to 2026-01-25, CC0) [7] and, following task instructions, exclude the USA.

Resolution. We adopt the finest resolution available in the SCI layer files: **NUTS 3** for EU countries (via GISCO 2024 boundaries [4]) and **GADM level 1** for all others (GADM v4.1 [5]). The SCI data do not provide sub-national codes at GADM level 3; GADM 1 is therefore the highest resolution accessible outside Europe.

Construction. From the raw layer CSVs we retain only *within-country* edges, drop self-loops, keep one edge per unordered pair, and sum duplicate `scaled_sci` values. Geographic coordinates (EPSG:4326) are obtained from boundary-polygon representative points. The resulting global deliverable contains $N = 3\,040$ nodes and $E = 134\,016$ edges across 99 countries; coordinate coverage is $\sim 98\%$ of nodes.

2.2 | Completeness and weighted perspective

A key observation is that *every* within-country graph is **complete**: the SCI dataset reports a weight for every pair of regions, so $E = \binom{N}{2}$ and density $= 1$ for all 99 countries (Fig. 2.1, left). Consequently, standard unweighted metrics are uninformative: $P(k) = \delta_{k,N-1}$, $C = 1$, and modularity $Q = 0$. All meaningful structure resides in the *weights*; the remainder of the analysis is therefore weighted.

Edge-weight distribution. Within each country we normalise weights by the maximum ($\hat{w}_{ij} = w_{ij}/w_{\max}$) and pool all edges across the 99 countries. The resulting

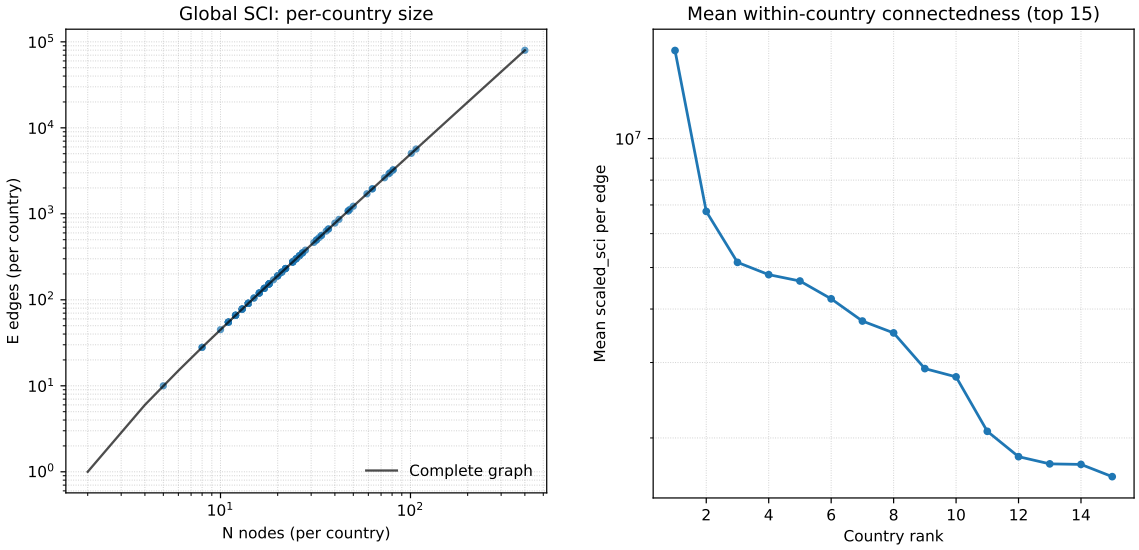

Figure 2.1: Left: edges versus nodes per country (log–log); the black curve is the complete-graph reference $E = N(N-1)/2$, confirming density $= 1$ for all countries. Right: mean within-country `scaled_sci` per edge versus country rank (top 15).

CCDF (Fig. 2.2, left) spans roughly four decades with a heavy tail: most edges carry low relative weight while a few region pairs are orders of magnitude more connected.

Node strength and Gini coefficient. The strength of node i is $s_i = \sum_j w_{ij}$. We summarise within-country strength heterogeneity via the Gini coefficient $G \in [0, 1]$ (Fig. 2.2, right). Values range from $G \approx 0.07$ (Japan, very homogeneous) to $G \approx 0.35$ (UK, dominated by London); the colour encodes mean strength, showing that heterogeneity is not simply a size effect.

2.3 | Weighted clustering

For complete graphs the unweighted clustering coefficient is trivially 1. We therefore compute the *weighted* clustering of Onnela et al. [8]:

$$C_i^w = \frac{1}{s_i\,(k_i - 1)} \sum_{j,h} \left(\hat{w}_{ij}\,\hat{w}_{ih}\,\hat{w}_{jh}\right)^{1/3},$$

where $\hat{w}$ is the max-normalised weight. C^w equals 1 only when all triangle weights are identical (perfectly homogeneous connectivity); heterogeneous weights lower it.

Fig. 2.3 (left) shows $\langle C^w \rangle$ per country (computed for countries with $N \leq 120$ for tractability). Russia, Japan, and Uganda ($C^w \gtrsim 0.89$) exhibit nearly uniform regional connectivity, whereas the UK ($C^w \approx 0.39$) is strongly London-centric. The weight matrix of Italy (Fig. 2.3, right) visualises the block structure typical of countries with a few dominant metropolitan areas.

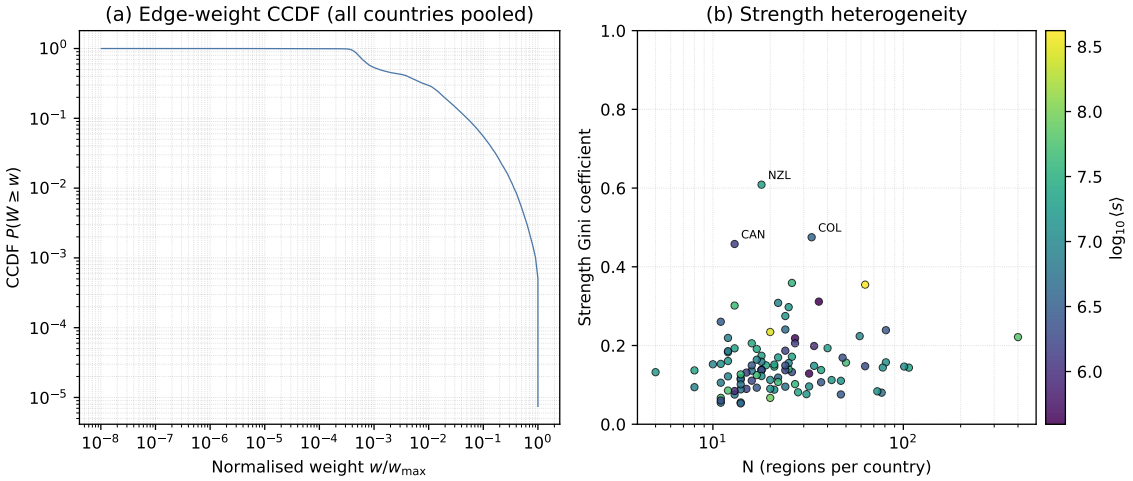

Figure 2.2: Left: CCDF of the max-normalised edge weight pooled across all 99 countries. Right: strength Gini coefficient versus network size; colour indicates $\log_{10}\langle s \rangle$.

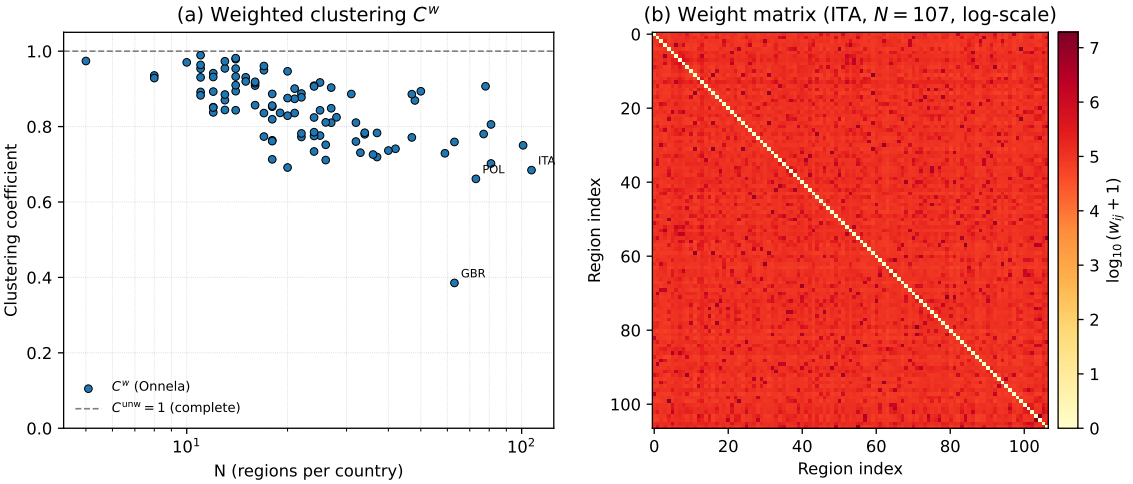

Figure 2.3: Left: weighted clustering $\langle C^w \rangle$ versus N; dashed line marks $C^{\text{unw}} = 1$. Right: log-scaled weight matrix for Italy ($N = 107$, NUTS 3 regions).

3 | Bibliography

[1] AI and Data for Good at Meta. Social connectedness index. https://ai.meta.com/ai-for-good/datasets/social-connectedness-index/, 2026. [Accessed 04-Feb-2026]. Reference period: 2025-12-26 to 2026-01-25. Updated: 2026-01-29.

[2] Eric Bonabeau. Sandpile dynamics on random graphs. *Journal of the Physical Society of Japan*, 64(9):327–336, 1995. doi: 10.1143/JPSJ.64.327.

[3] Charles D. Brummitt, Raissa M. D'Souza, and E. A. Leicht. Suppressing cascades of load in interdependent networks. *Proceedings of the National Academy of Sciences*, 109(12):E680–E689, 2012. doi: 10.1073/pnas.1110586109.

[4] European Commission, Eurostat (GISCO). Nuts regions (2024) - gisco distribution (level 3, epsg:4326). https://gisco-services.ec.europa.eu/distribution/, 2024. [Accessed 04-Feb-2026]. GeoJSON endpoint used: NUTS_RG_01M_2024_4326_LEVL_3.

[5] GADM. Gadm database of global administrative areas (version 4.1). https://gadm.org/, 2025. [Accessed 04-Feb-2026]. Shapefile downloads mirrored at https://geodata.ucdavis.edu/gadm/.

[6] K.-I. Goh, D.-S. Lee, B. Kahng, and D. Kim. Sandpile on scale-free networks. *Physical Review Letters*, 91:148701, 2003. doi: 10.1103/PhysRevLett.91.148701.

[7] Humanitarian Data Exchange (HDX). Facebook social connectedness index. https://data.humdata.org/dataset/social-connectedness-index, 2026. [Accessed 04-Feb-2026]. Coverage: 178 countries. Reference period: 2025-12-26 to 2026-01-25. Updated: 2026-02-07. License: CC0.

[8] J.-P. Onnela, J. Saramäki, J. Kertész, and K. Kaski. Intensity and coherence of motifs in weighted complex networks. *Physical Review E*, 71:065103, 2005. doi: 10.1103/PhysRevE.71.065103.